Formation of stable non-gaussian velocity distribution on gravitational collapse and in merging process

Kanaeda Naoko[1], Masahiro Morikawa[2]

Department of Physics, Ochanomizu University, 2-1-1 Ohtuka, Bunkyo, Tokyo, 112-8610

(Received 29 May 2003)

Abstract

The results of collisionless n-body simulations are presented. We discuss the formation of the velocity distribution in collisionless n-body 3-dimensional system using GRAPE5. We caluculate two models, a spherical collapse and a cluster collision, and observe stable non-gaussian velocity distributions which are well fitted by equall-weight superposition of thermal distributions with various temperatures (DT). As for the spherical model, the velocity distributions are DT distyributions in all cases provided that the initial virial ratio is less than 0.23. As for the cluster collision model, the velocity distributions are in-isotropic and depnends on axis. These non-gaussian velocity distributions are formed well before the thermallization of the systems and stably persist for all the time within our numerical calculations. The appearance of non-Gaussian velocity distributions strongly depends on the initial virial ratio but have no connection with other parameters such as softening parameter, initial configrations or velocity distributions.

1 Introduction

The galaxies are typical self-gravitating systems (SGS); the system of particles which interact via their own gravity. To clarify the evolution of SGS is an important issue to understand our universe. Among several kinds of galaxies, we concentrate on the ellipticall galaxies which are thought to be collision-less systems. They reflect genuin properties of gravity without fluid dynamics nor heat transfer processes.

It is widely accepted till today that the luminosity profile of observed elliptical galaxies obeys the de Vaucouleur law [4][5][6]. This ovservational fact indicates that the elliptical galaxies presumably reach the equilibrium state and as a result, their luminosity profile realized. Then, this observation gives rise to a question how we can explain a mechanism which cause macroscopic properties like luminosity profile in equilibrium state of SGS. It means whether we have statistical method which can apply to SGS or not.

It is natural to expect to apply the Boltzmann-Gibbs statistics to SGS, but this system doesn't come up to our expectation because of some characteristic propeties owing to long range force, for examples, a divergence of macroscopic properties in thermodynamic limit or being unstable in thermal equilibrium[2][3]. In addition, the statistical method of SGS- the prescription that reduces the huge (6N-1) degrees of freedom to a few of them - has not been found till today. Then, even if we can see that the elliptical galaxies stay in equilibrium state but we do not know how the universal form of luminosity profile were established.

However, we can judge whether the elliptical galaxies are thermalized or not by calculating their two-body relaxation time t_{relax}[3][13]. The t_{relax} of elliptical galaxies is 10^{14}years. Then, the two-body relaxation time of the elliptical galaxies is 10,000 times longer than the age of the Universe(10^{10}years) and we see that elliptical galaxies are far from thermal equilibrium though they seem to be in equilibrium state. Then we expect that there exist a quasi-equilibrium state before SGS are thermalized. The relaxation process towards the quasi-equilibrium state is called 'collisonless relaxation' and themalized system is called 'collisional system'[3].

[1]kanaeda@degway.phys.ocha.ac.jp
[2]hiro@phys.ocha.ac.jp

The mechanism which cause the collisionless relaxation is first studied by Lynden Bell[1]. He proposed the concept violent relaxation - a relaxation process caused by the accumulation of a variance of the energy by two body encounter between distant particles - providing a initial condition of SGS are far from dynamical equilibrium (therefore, the violent relaxation is a characteristic nature of long range force). The characteristic time scale of the violent relaxation is free fall time of the system which is much shorter than two body relaxation time.

To clarify the details of the violent relaxation process, a number of n-body simulations have been performed. As a result, the stable macroscopic properties realized after violent relaxation depends on a initial conditions i.e. the violent relaxation incompletely occurs. Thus, we have to clarify what kind of macroscopic properties are realized depending on initial conditions in collisionless system.

The density profile in open 3-D collisionless system has been studied by using n-body simulation starting from a various initial conditions[7][8][9][10]. The propose of these studies are to explain the mechanism which produced the observed luminocity profile which is the projected density profile providing that we define the luminosity-mass raito. However, the velocity distribution, which is usually not observed, was not an interesting object. Therefore it has hardly been studied numerically except the pair-wise velocity distribution (this can be observed).

However by using a simple n-body model, the velocity distribution has studied from a viewpoint of statistical nature of phase spase in SGS. The SGR model(self gravitating ring model) is the ring on which the particles are constrained and they interatct via 3-D gravity. In this sysytem, the stable non-gaussian distribution ehich is fitted by Lorenzian distribuiton was found[14]. As an other example, we introduced HMF model which is the system of paritcles which interact with each other in a well of potential. The non-gaussian distribution were observed in quasi-equilibrium state and after the system is thermalized it changes into gaussian. But, since these are one-dimentional models and the force is not gravity, these model are not realistic.

Then, we start our study from investigating what kind of velocity distribution of the collisionless open 3-D system realizes in quasi-equiribrium state by using n-body simulation interacting via gravity starting from the various initial conditions.

2 Simulation code and choice of initial conditions

2.1 Simulation program and algorithm

In this paper, we use GRAPE5 , special-propose numerical hard device for gravitating n-body simulation. We use the direct summation numerical code and employ the leap-flog integrator. The equation of motion governing the gravitational n-body system is,

$$\frac{d^2\boldsymbol{x}_i}{dt^2} = -G\sum_{i\neq j}^{N} m_j \frac{\boldsymbol{x}_i - \boldsymbol{x}_j}{(|\boldsymbol{x}_i - \boldsymbol{x}_j|^2 + \epsilon^2)^{\frac{3}{2}}}, \tag{1}$$

where m_i and $\boldsymbol{x}_i$ are the mass and the position of i-th particle respectively and ϵ is a softening parameter which is introduced to prevent the divergent forces when a distance between two particles goes to 0.

2.2 Scaling

In our simulation , we employ the following units, G=1 , M=$\frac{1}{N}$=1, R_{sys}=1.0. Here , G is the gravitational constant, M is the total mass of the system, N is the number of particles, R_{sys} is the characteristic scale of the system. Then the dynamical time of the system t_{dyn} becomes,

$$t_{dyn} = \sqrt{\frac{R_{sys}^3}{GM}} = 1.0. \tag{2}$$

We fix the softening parameter ϵ to be 2^{-8}(which is about 0.004).

2.3 Initial Condition

We perform two kinds of experiment, spherical collapse and cluster collision(the number of cluster is limited to be two) as simple models which cause the violent relaxation. Since we interested in what kind of velocity distribution is formed depending on the initial conditions, we simulate these two models changing them. We describe the details of initial conditions.

In the case of spherical collapse, initially we set a radius to R_{sys} and distribute the particles uniformly. The initial velocity distribution is gaussian. Added to these situation, we set the number of particles N as 4096 or 16384. In each case of N, we set the virial ratio as 0.0, 0.1, 0.2, 0.3 or 0.5. We denote the number of particles with 16384 by **S** and with 4096 by S(S means spherical collapse). We represent the virial ratio by suffix, for example $S_{0.0}$ indicates that N is 4096 and virial ratio is 0.0.

In the case of cluster collisions, a cluster means a sphere with radius R_{sys} in which half of the total particles in the system distribute uniformly and its velocity distribution is gaussian. Initially we put each cluster separately along x axis and the distance between the clusters is fixed to be 6 times R_{sys} in all runs. Furhter, we set the total number of particles in the system N as 4096 or 16384. In case N=4096, we set the virial ratio of each cluster as 0.2, 0.6, 1.0 or 1.4. In added to these runs, we calculate another one giving the finite angular momentum L_z with virial ratio of each cluster 1.0. In case N=16384, we set the virial ratio of each cluster as 1.0. We denote the number of particles with 16384 by **C** and with 4096 by C (C means cluster collision). We represent the virial ratio by suffix, for example $C_{0.2}$ indicates a run that N=4096 with virial ratio 0.2. We denote the run with finite L_z and virial ratio 1.0 by $\mathbb{C}_{1.0}$.

3 Simulation and results

3.1 Time evolution of the simulated models

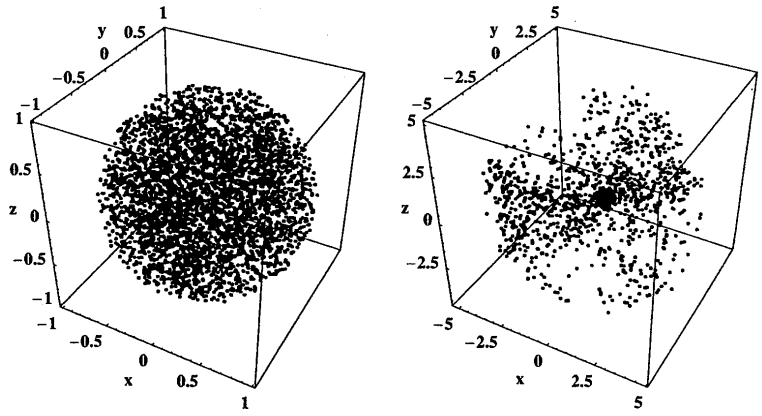

Figure 1: Snapshots in the (x, y, z) space for run $S_{0.0}$(spherical collapse of 4096 pariticles with initial virial raito 0.0). Each points in these boxies show the positions of particles. The left box shows a snapshot at t=$0.0t_{dyn}$. The right box shows a snapshot at t=$10.0t_{dyn}$

We report the time evolution of the system. Figure 1 are snapshots for run $S_{0.0}$. Each box shows positions of particles. The left box is a snapshot at $t = 0.0t_{dyn}$ and the right box is at $t = 10t_{dyn}$. At $t = 0.0t_{dyn}$, the particles are distributed uniformly but at $t = 1.2t_{dyn}$ they collapse. Soon after the collapse, some part of the particles are bounded gravitationally in the center of the system and the other part of the particles scatter into the outer part of the system(we call such a structure core-halo structure). This structure is stable during the calculation time $100t_{dyn}$.

Figure 2 shows snapshots for run $C_{0.2}$. The left box shows a snapshot at $t = 0.0t_{dyn}$ and the right box at $t = 40t_{dyn}$. The clusters are approaching with each other along the x axis and collide at $t = 20t_{dyn}$. After the collision, we find the core-halo structure and it is stable during the calculation time.

The error of the total energy is smaller than one percent in all runs.

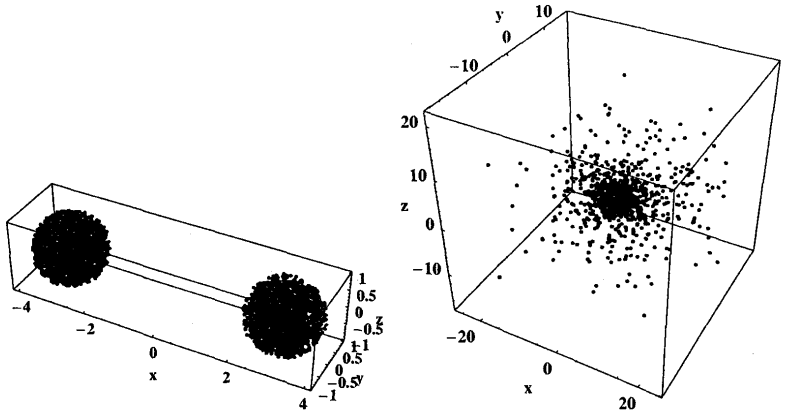

Figure 2: Snapshots in the (x, y, z) space for run $C_{0.2}$(cluster collision with 4096 particles and the initial virial raito of each cluster 0.2). Each points in these boxies show the positions of particles. The left box shows a snapshot at t=$0.0t_{dyn}$. The right box shows at t=$40.0t_{dyn}$

3.2 Time evolution of virial raito and velocity dispersion

We describe the core-halo structure seems to have been stable during the calculation time. Then, we investigate how the other properties evolve after core-halo structure is formed. We investigate the time evolution of the virial ratio and the velocity dispersion of the system.

Figure 3 shows the time evolution of virial ratio and the velocity dispersion. The left two frames show the time evolution of virial ratio and the right two frames show the time evolution of velocity dispersion. Top two frames show the results for run $S_{0.0}$ and bottom two frames for run $C_{1.0}$. They seeme to be stable after the formation of core-halo structure.

3.3 The stable velocity distribution depending the initial conditions

Now we discusse the issue that what kind of velocity distribution is formed depending on the initial conditions. We investigate the velocity distribution after stable core-halo structure is formed because we interested in statitical properties in stable state - especially for quasi-equiribrium state caused by the violent relaxation.

We apply the chi-square analysis for earching the best fitting function. We first employ the gaussian and the exponential fitting functions. The reason why we choose the exponential fitting function is as follows. When we apply $f(v) = aexp(-b|v|^{\alpha})$ fitting, the observed velocity distribution by means of the least square method, α is best fitted by 1.07 in the case of spherical collapse provided thst the virial ratio is amall. Next we apply another fitting function which is composed as the equall weight superposition of gaussian functions (DT=democratic temperature). The explicite form is given by

$$f(v_i) = a\int_0^{T_0} exp(-v_i^2/2T)dT = a[\sqrt{\frac{2T_0}{\pi}}e^{-\frac{v_i^2}{2T_0}} - |v_i|[1 - Erf(\frac{|v_i|}{\sqrt{2T_0}})]], \tag{3}$$

where suffix i is x, y or z and T means temperature, a and T_0 are fitting parameters. This form of function is suggested by the fact that in our numerical calculations, the mean temperature (defined by averaging the velocity dispersions at the mass fraction $M(r)$ at radius r) shows linear dependence: $T \propto M(r)$.

In Figure 4, the upper frame shows the observed velocity distribution for the run $S_{0.0}$, the spherical collapse model with initial virial ratio 0.0. The lower frame shows a velocity distribution for the run $C_{1.0}$, the cluster collision with initial virial ratio 0.2. These velocity distribution have been stable (it means a deviation of fitting parameter from its mean value has stayed within a few percent of its mean value) during calculation time after the core-halo structure are formed. This velocity distribution can not be fitted by simple gaussian distribution on the whole part of f(v), especially v close to 0. On the other hand, these velocity distributions seem to be well fitted with DT distribution or exponential function

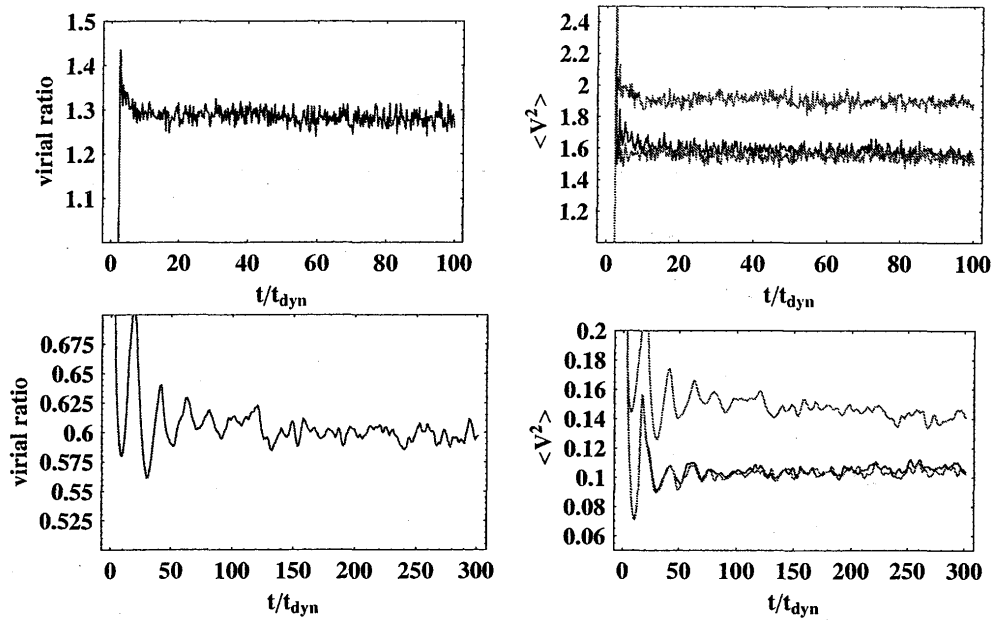

Figure 3: Time evolution of the virial raito and velocity dispersion for run $S_{0.0}$ and $C_{1.0}$ ($S_{0.0}$ is the spherical collapse of 4096 particles with the initial virial ratio 0.0 and $C_{1.0}$ is the collision of two clusters whose size is 2048 and the initial virial raito 1.0). Two left frames show the virial ratio and two right frames show velocity dispersion. Top two frames show the results for run $S_{0.0}$ and bottom two frames for run $C_{1.0}$. In left frames, vertical axis represents the virial ratio and horizonal axis represents t/t_{dyn}. In right frames, vertical axis represents velocity dispersion $< v_x^2 >$, $< v_y^2 >$ and $< v_z^2 >$ and horaizonal axis time t/t_{dyn}.

than gaussian. Such non-gaussian velocity distributions are also observed for the run $S_{0.0}$, $S_{0.1}$, $S_{0.2}$, $\mathbf{S}_{0.0}$, $\mathbf{S}_{0.1}$ and $\mathbf{S}_{0.2}$ (spherical collapse) and all cases of cluster collision.

Now, we quantitatively examine the above fittings by means of the chi-square test. In figure 5, the upper frame shows the time evolution of the chi-square value for run $S_{0.0}$ and the lower frame shows for run $C_{1.0}$. The black boxs, gray boxs and black triangles represent exponential, gaussian and DT distributions respectively. We find that the velocity distributions are best fitted by DT distribution.

Figure 6 shows time evolution of the fitting parameter(velocity dispersion) for the run $C_{1.0}$. The black boxs, gray boxs and black triangles represent exponential, gaussian and DT distributions respectively. These parameters seem to have been stable during the calculation time.

Table 1 summarizes the best fitting functions. In the case of spherical collapse, for the initial virial ratio 0.0, 0.1 or 0.2, the velocity distribution is non-gaussian and is best fitted by DT distribution, however in the case for 0.3 and 0.5, the velocity distribution becomes gaussian regardless of the number of particles. In the case of cluster collision, the velocity distribution is best fitted by DT distribution in $C_{0.2}$, $C_{0.6}$, $C_{1.0}$ and $\mathbf{C}_{1.0}$ but it depends on axis. For run $C_{1.4}$, the velocity distribution is fitted by the exponential function. For the run $\mathbb{C}_{1.0}$, $f(v_x)$ and $f(v_y)$ are gaussian and $f(v_z)$ is DT distributions. It means that the velocity distribution on the direction of rotating plane is gaussian and that on the direction of rotating axes is non-gaussian. The reason has not yet been clarified at present.

3.4 The relaxation time

We calculate the two-body relaxation time in order to check whether this system is thermallized or not when the non-gaussian velocity distitbution are found. The two-body relaxation time is expressed by,

$$t_{relax} = 0.1 \frac{N}{Log[N]} t_{dyn}, \tag{4}$$

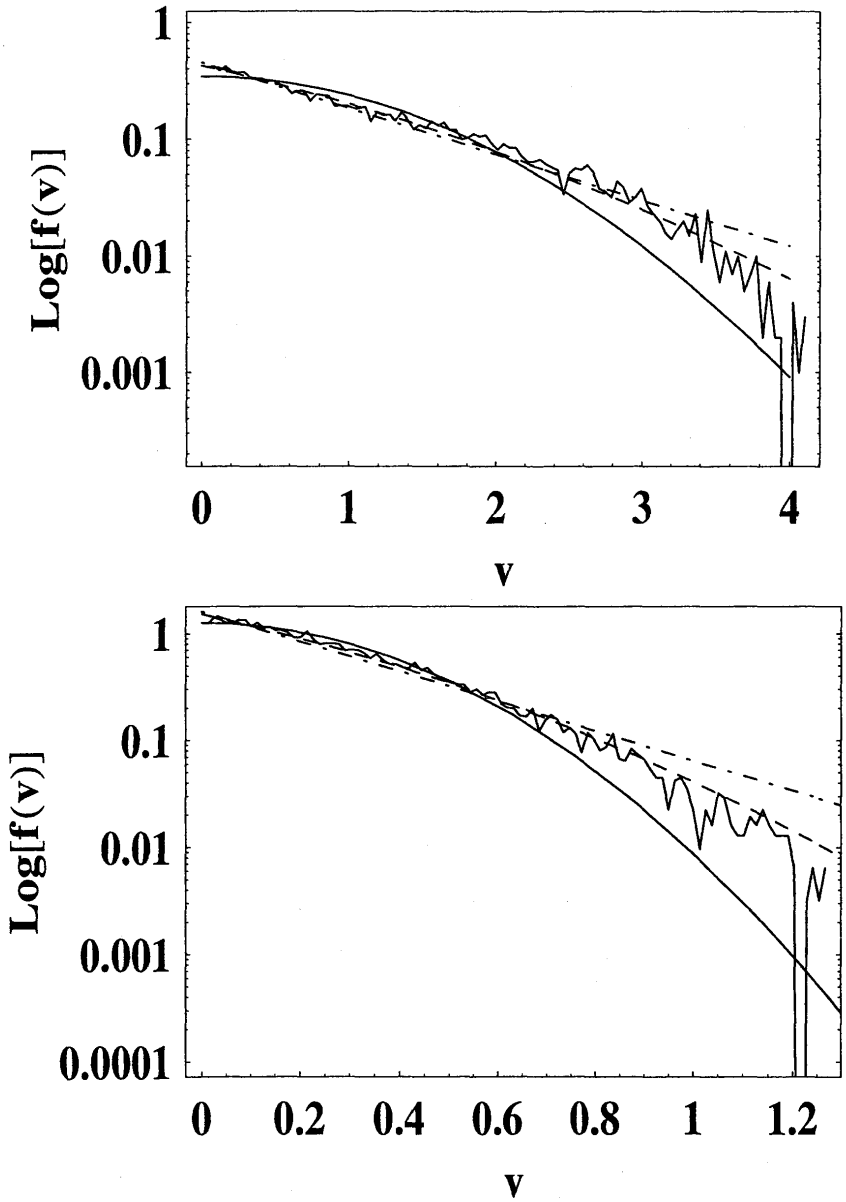

Figure 4: Loglinear plot of the observed stable non-gauss velocity distribution for the run $S_{0.0}$ (spherical collapse of 4096 particles with initial virial ratio 0.0) and $C_{1.0}$(cluster collision with the number of particles and virial ratio of each cluster are 2048 and 0.0) at t=$100t_{dyn}$. Vertical axis represents the logarism of the velocity distribution function. Horizonal axis represents velocity. A solid line represents the best fitting gaussian function. The chain line represents the best fitting exponential function. A broken line represents the best fitting DT distribution.

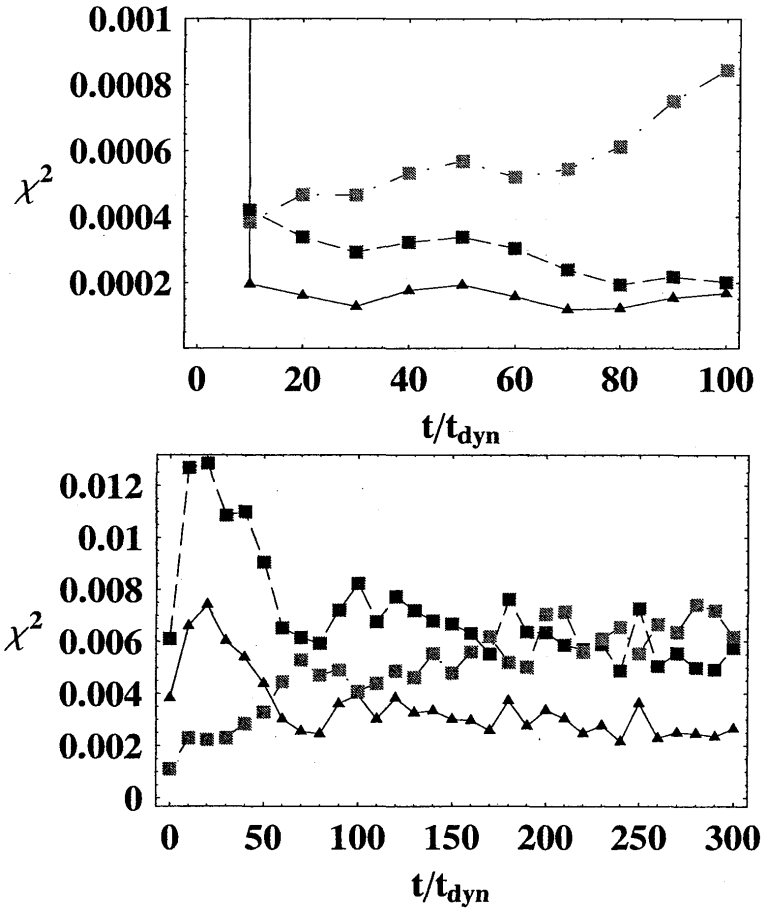

Figure 5: Time evolution of chi-square value for run $S_{0.0}$, $C_{1.0}$($S_{0.0}$ is spherical collapse of 4096 particles with virial ratio 0.0 and $C_{1.0}$ is cluster collision with the number of particles and virial raito of each cluster are 2048 and 1.0). Vertical axis shows the chi-square value and the horizontal axis shows time t/t_{dyn}. The black boxs, gray boxs, and black triangles show the chi-square values for the exponential, gaussian, and DT fittings respectively. The chi-square values for DT fitting are the order of 10^{-4} for run $S_{0.0}$ and the order of 10^{-3} for run $C_{1.0}$.

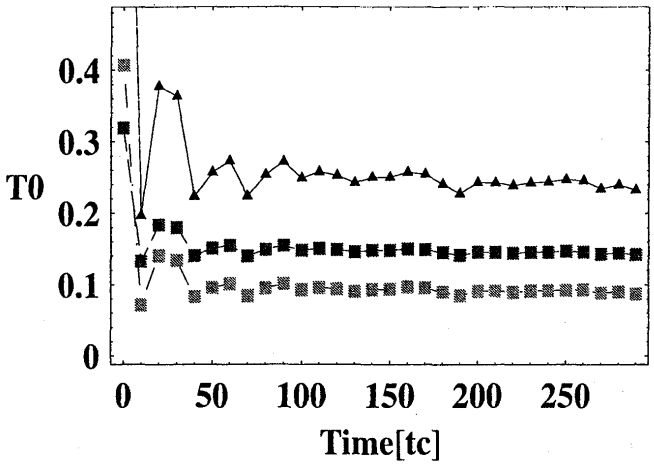

Figure 6: Time evolution of velocity dispersion for run $C_{1.0}$ (cluster collision with the number of particles and virial ratio of each cluster 2046 and 1.0). Vertical axis shows the fitting velocity dispersion and horaizonal axis shows t/t_{dyn}. The black boxs, gray boxs and black triangles represents exponential, gaussian and DT fittings respectively.

where N is the number of the particles.

In the case of spherical collapse, initially t_{relax} is about $130t_{dyn}$ if N is 4096 and about $390t_{dyn}$ if N is 16384. After the collapse, however, the radius of the system contracts and becomes ten percent of the initial value. Then, t_{relax} after the collapse is about $4.2t_{dyn}$ for N=4096 and is about $11.7t_{dyn}$ for N=16384. Therefore the system is collisionless before $t = 5.4t_{dyn}$ for N=4096 and before $t = 13.9t_{dyn}$ for N=16384 since the collapse occures at $t = 1.2t_{dyn}$. From Figure 5 we can not know the details of the chi-square value between $0t_{dyn}$ and $10t_{dyn}$, so we need to know the details. Figure 7 shows the time evolution of the chi-square value from $t = 1t_{dyn}$ to $10t_{dyn}$ for run $S_{0.0}$(top frame) and run $\mathbf{S}_{0.0}$(bottom frame). We can find that the non-gaussian velocity distribution are found when the system is collisionless and also found after it is thermallized.

We estimate the two-body relaxation in the case of cluster collision. After the collision at $t = 20t_{dyn}$, the radius of the system does not change, so the t_{relax} is about $t = 150t_{dyn}$ for N=4096. From Figure 5, we find the non-gaussian velocity distribution are found before and after the system is thermallized.

3.5 Further calculation and initial conditions

In section 3, we presente the result of simulation of our models, spherical collapse and cluster collision, and observed the stable non-gaussian velocity distribution fitted by DT distribution. In case of spherical collapse, this non-gaussian distribution appears if the virial ratio is 0.0, 0.1 or 0.2. In case of cluster collision, non-gaussian distribution is observed reagradless of the initial virial ratio.

In order to check the universality of the above results, we should further examine the following points. First, we should examine that the softening parameter does not affect the simulational results. The simulational results would not be correct if the considerable particles interact within a scale of the softening parameter. Second, we should examine whether the non-gaussian velocity distribution depends on the initial properties such as the particle distributions or velocity distributions or not. These initial properties may lead to non-gaussian velocity distribution. Third, as for spherical collapse, we should investigate where the ciritical virial ratio (under which the non-gaussian distribution is found) exits. Forth, we are interested in how long the non-gaussian distribution stably persists.

To answer the first point, we investigate the number of the particles whose relative distance is less than the softening parameter for run $S_{0.0}$ and $C_{0.2}$. As for the second point, we change the softening parameter from 2^{-9} to 2^{-11} for run $\mathbf{S}_{0.0}$ and check whether the result depends on this change or not. We denote these simulation $\mathbf{S}_{0.0}$ by ,for example, $\mathbf{S}_{0.0}(\epsilon = 2^{-9})$. Furthermore, we change the initial velocity or position distribution function for run $S_{0.1}$ and $C_{1.0}$. We change the position distribution in sphere or a

RUN	$f(v_x)$	$f(v_y)$	$f(v_z)$
$S_{0.0}$	DT	DT	DT
$S_{0.1}$	DT	DT	DT
$S_{0.2}$	DT	DT	DT
$S_{0.3}$	GAUSS	GAUSS	GAUSS
$S_{0.5}$	GAUSS	GAUSS	GAUSS
$\mathbf{S}_{0.0}$	DT	DT	DT
$\mathbf{S}_{0.1}$	DT	DT	DT
$\mathbf{S}_{0.2}$	DT	DT	DT
$\mathbf{S}_{0.3}$	GAUSS	GAUSS	GAUSS
$\mathbf{S}_{0.5}$	GAUSS	GAUSS	GAUSS
$C_{0.2}$	DT	EXP	EXP
$C_{0.6}$	DT	DT	DT
$C_{1.0}$	DT	DT	DT
$C_{1.4}$	EXP	EXP	EXP
$\mathbf{C}_{1.0}$	DT	DT	DT
$\mathbb{C}_{1.0}$	GAUSS	GAUSS	DT

Table 1: Best fitted functions for all runs. $f(v_x)$, $f(v_y)$ and $f(v_z)$ represent the distribution function of the velocity along the x, y and z axis. DT represents the DT distribution. GAUSS represents the gaussian function. EXP represents exponential function. The character S means spherical collapse and the character C means cluster collision. Suffix represents the initial virial ratio of the system(S) or a cluster(C). $\mathbb{C}_{1.0}$ represents the cluster collision giving z-component of angular momentum.

cluster from uniformal distribution to the density distribution which is proportional to $r^{-0.5}$ for run $S_{0.1}$ and $C_{1.0}$. Next, we change the velocity distribution in a sphere or in a cluster from gaussian to uniform distribution for run $S_{0.1}$ and $C_{1.0}$. We denote the simulation $S_{0.1}$ and $C_{1.0}$ changing position distribution by $S_{0.1}(r^{-0.5})$ and $C_{1.0}(r^{-0.5})$ respectively. We denote the simulation $S_{0.1}$ and $C_{1.0}$ changing the velocity distribution by $S_{0.1}$(uniform) and $C_{1.0}$(uniform) respectively. As for the third point, we calculate the run $\mathbf{S}_{0.0}$ changing the virial ratio from 0.17 to 0.29 with interval 0.02. In the subsection 3.3, we have confirmed that the non-gaussian velocity distribution is observed if the initial virial ratio is 0.0, 0.1 and 0.2 and gaussian if regardless of the number of particles. Then we estimate the ciritical initial virial ratio, below which the DT distribution appears, exists between 0.2 and 0.3. We denote these runs by same way as in 2.2. As for the forth point, we calculate run $C_{1.0}$ for $10^3 t_{dyn}$. We denote this long simulation by $C_{1.0}(t = 10^3 t_{dyn})$.

3.6 Simulational result

We count the number of particles within a softening parameter during the calculation for run $\mathbf{S}_{0.0}$ and $C_{0.2}$, virial ratio of $\mathbf{S}_{0.0}$ and $C_{0.2}$ is the lowest in the spherical collapse or the cluster collision. We have fixed the softening parameter 2^{-8}. As a result, the number of particles interact within the scale of softening parameter is almost 0 or 1 during the calculation time.

Table 2 summarizes the result of the velocity distribution for run $\mathbf{S}_{0.0}(\epsilon = 2^{-9})$, $\mathbf{S}_{0.0}(\epsilon = 2^{-10})$ and $\mathbf{S}_{0.0}(\epsilon = 2^{-11})$. We can not find out the connection between the appearence of non-gaussian velocity distribution and the softening parameter.

Table 3 summarizes the result for run $S_{0.1}(r^{-0.5})$, $S_{0.1}(uniform)$, $C_{1.0}(r^{-0.5})$ and $C_{1.0}(uniform)$. We can not find out the connection between the appearence of non-gaussian velocity distribution and the initial density profiles.

Table 4 summarizes the run $S_{0.17}$, $S_{0.19}$, $S_{0.21}$, $S_{0.23}$, $S_{0.25}$, $S_{0.27}$ and $S_{0.29}$. The non-gaussian velocity distribution fitted with DT distribution are observed for run $S_{0.17}$, $S_{0.19}$ and $S_{0.21}$. It means the velocity distribution is non-gaussian provided the virial ratio is 0.17, 0.19, 0.21 and 0.23. For the run $S_{0.29}$, the best fitting function cannot be determind; both gaussian and DT distributions fit the data with almost the same chi-square value during the calculation time. For the run $S_{0.29}$, the velocity distribution is

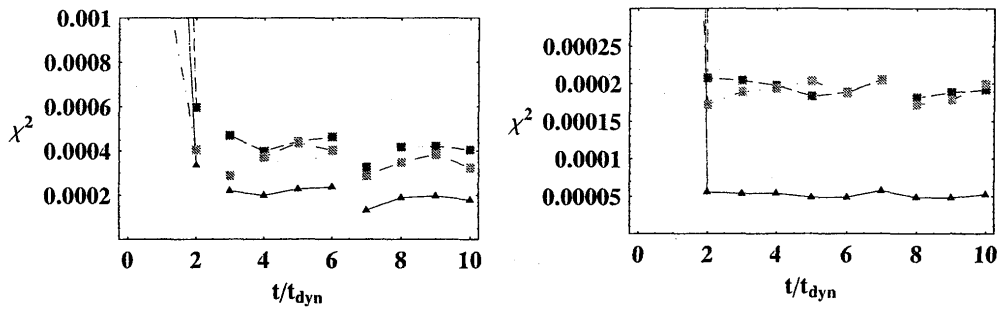

Figure 7: The time evolution of the chi-square value before $t = 10t_{dyn}$. The top frame shows for run $S_{0.0}$ from $t = 1t_{dyn}$ to $10t_{dyn}$ and the bottom frame shows for run $\mathbf{S}_{0.0}$ from $t = 1t_{dyn}$ to $10t_{dyn}$($S_{0.0}$ is spherical collapse of 4096 particles with virial ratio 0.0 and $\mathbf{S}_{0.0}$ is spherical collapse of 16384 particles with viral ratio 0.0). The black boxs show the chi-square value for the exponential fitting. The gray boxs show the chi-square values for the gaussian fitting. The black triangles show the chi-square values for DT fitting. The chi-square value of DT model is the order of 10^{-4} in both runs.

RUN	$f(v_x)$	$f(v_y)$	$f(v_z)$
$\mathbf{S}_{0.0}(\epsilon = 2^{-9})$	DT	DT	DT
$\mathbf{S}_{0.0}(\epsilon = 2^{-10})$	DT	DT	DT
$\mathbf{S}_{0.0}(\epsilon = 2^{-11})$	DT	DT	DT

Table 2: Observed velocity distribution function changing the softening parameter. $f(v_x)$, $f(v_y)$ and $f(v_z)$ represent the distribution function of the velocity along x, y and z axis respectively. DT represents the DT distribution. $\mathbf{S}_{0.0}$ repsents spherical collapse of 16384 particles with virial ratio 0.0 and ϵ in brackets means softening parameter.

clearly gaussian. Therefore, we conclude that the critical virial ratio exists between 0.21 and 0.23.

Figure 8 shows the time evolution of the chi-square value for run $C_{1.0}(t = 10^3_{dyn})$. We find that the non-gaussian velocity distribution is observed during this calculation time $10^3 t_{dyn}$.

4 conclusion

In this paper, we have investigated the formation of a stable velocity distribution depending on the initial conditions using GRAPE5 in order to clarify the statistical nature in collisionless open 3-D system.

We have calculated the spherical collapse and the cluster collison as simple models of collisionless system. These systems form the core-halo structure soon after the collpse or the collision and it has been stable during the calculation time. These systems reach collisionless relaxation and move to the next

RUN	$f(v_x)$	$f(v_y)$	$f(v_z)$
$S_{0.1}(r^{-}0.5)$	DT	DT	DT
$S_{0.1}(uniform)$	DT	DT	DT
$C_{1.0}(r^{-0.5})$	DT	DT	DT
$C_{1.0}(uniform)$	DT	DT	DT

Table 3: Velocity distribution function changing initial properties, velocity and position distribution function. $f(v_x)$, $f(v_y)$ and $f(v_z)$ represent the distribution function of the velocity along x, y and z axis. DT represent the DT model. $S_{0.1}$ means spherical collapse of 4096 particles with virial ratio 0.0 and $C_{1.0}$ means cluster collision with the number of particles and virial ratio of each cluster are 2048 and 1.0. $r^{-0.5}$ and uniform in brackets represent the initial density profile.

RUN	$f(v_x)$	$f(v_y)$	$f(v_z)$
$S_{0.17}$	DT	DT	DT
$S_{0.19}$	DT	DT	DT
$S_{0.21}$	DT	DT	DT
$S_{0.23}$	DT or GAUSS	DT or GAUSS	DT or GAUSS
$S_{0.25}$	DT or GAUSS	DT or GAUSS	DT or GAUSS
$S_{0.27}$	DT or GAUSS	DT or GAUSS	DT or GAUSS
$S_{0.29}$	GAUSS	GAUSS	GAUSS

Table 4: Velocity distribution function changing the virial ratio from 0.17 to 0.29. $f(v_x)$, $f(v_y)$ and $f(v_z)$ represent the distribution function of the velocity along x, y and z axis respectively. DT represents the DT distribution. Gauss represents the gaussian function. Character S means spherical collapse of 4096 particles and suffix shows virial ratio.

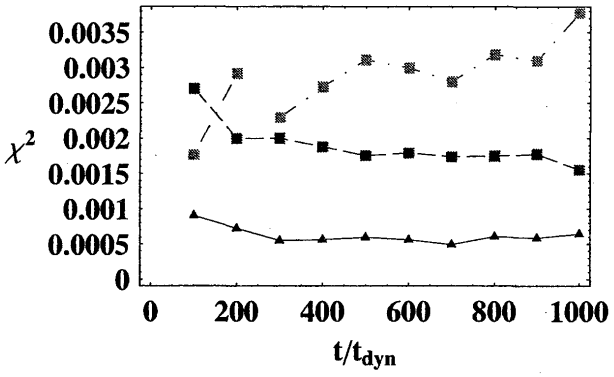

Figure 8: The time evolution of the chi-square value for run $C_{1.0}(t = 10^3_{dyn})$($C_{1.0}$ is cluster collision with the number of particles and virial ratio of each cluster are 2048 and 1.0. The $t = 10^3_{dyn}$ in brackets shows calculation time). Vertical axis represents the chi-square value and horaizonal axis represents time t/t_{dyn}. The black boxs show the chi-square value for the exponential fitting. The gray boxs show the chi-square value for the gaussian fitting. The black triangles show the chi-square value for DT fitting. The chi-square value for DT fitting is the order of 10^{-4}.

stage of the collisional relaxation.

In both models, we have observed the stable non-gaussian velocity distribution fitted with DT distribution depending on initial conditions. As for the spherical model, we set the virial ratio 0.0, 0.1, 0.2, 0.3, 0.5 and as for each case, the number of particles was 4096 and 16384. In conclusion, the velocity distributions are non-gaussian provided that the virial ratio is 0.0, 0.1 and 0.2 regardless of the number of particles. As for the cluster collision, we set the virial ratio 0.2, 0.6, 1.0 and 1.4 fixing the number of particles to 4096. We separate two clusters along with x axis and set null angular momentum. Besides, we changed the number of particles to 16384 and give the z-component of the angular momentum. In conclusion, the stable non-gaussian distribution are observed in all runs.

Next, we have checked four points. First, we have confirmed that the particles which interact within the scale of the softening parameter are rare. Therefore, the effect of the softening parameter can be ignorable in our simulations. Second, we have checked whether the initial properties such as the softening parameter or initial velocity and position affect the formation of the non-gaussian velocity distribution. As a result, we have found no such effects on the appearance of non-gaussian distributions. Third, we have tried to find out the critical value of the initial virial ratio. We have changed the initial virial ratio from 0.17 to 0.29 with the interval 0.02. This choice is because we previously found that the velocity distribution is non-gaussian in runs whose virial ratio is 0.0, 0.1 or 0.2 and gaussian in runs whose virial ratio is 0.3 or 0.5. It was expected that the critical value exists between 0.2 and 0.3. As a result, the

velocity distribution is non-gaussian providid that the virial ratio is between 0.16 and 0.21, however from 0.23 to 0.27, we can not determine the best fitting function; both DT distribution and guassian dsitribution give almost the same chi-square values. In case the virial ratio is 0.29, the distribution function is clearly gaussian. So, we have concluded that in spherical collape, the critical virial ratio exist between 0.21 and 0.23. Forth, we have calculated the cluster collision and have found that the non-gaussian velocity distribution has been stable till 1000 dynamical time.

In this paper, we have found that stabe non-gaussian velocity distribution function exists in the collisionless relaxation process depending on the initial conditions. This distibution is well fitted by DT distribution or exponential functions. In case of spherical collapse the DT distribution is formed provided that the virial ratio is less than 0.23. In case of cluster colision, this DT distribution is found in wide range of initial conditions.

Acknowledgement

We would like to thank Osamu Iguchi and Yasuhide Sota for their valuable comments, suggestions, and constant supports. We also thank Takayuki Tatekawa and Akika Nakamichi for their advice and discussions on N-body code. We also thank Naoteru Gouda for useful comments.

The simulational program we use in this paper owes to E. Kokubo. We also would like to thank him for given N. K. a chance to attend a cource of spring school for GRAPE sponsored by National Astronomical Observatory in Mitaka.

References

[1] Lynden Bell, 1967, Mon.Not.R.Astr.Soc 136, 101-121

[2] Lynden-Bell and Rodger Wood, 1968, Mon.Not.R.astr.Soc, 138, 495-525

[3] James and Binney & Scotto Tremaine, 1987, Glactic Dynamics, Princeton

[4] G de Vaucouleurs, 1953, MNRAS.113.134D

[5] John Kormendy, 1977, Apj, 218, 333K

[6] G. Fasano and M. Fillippi, 1998, Astron.Astrophys.Suppl.Ser.129, 583-591

[7] Van Albada, 1982, MNRAS, 136, 101

[8] S.J.Aarseth and James Binney, 1978, MNRAS.209.15

[9] A.May and T.S. Albada, 1984, MNRAS.209.15

[10] Jens Verner Villumsen, 1984, Apj, 284, 75V

[11] David Merrit, Scott Tremaine and Doug Johnstone, 1989MNRAS, 236, 829M

[12] Ch. Theis and R. Spurzem, 1999, Astron.Astrophys., 341, 361

[13] Chandrasekhar, Principles of Stellar Dynamics

[14] W.H.Zurek, 1994, Apj, 431, 559Z

[15] Somak Raychaudhury and William C. Saslaw, 1996, Apj, 461, 514R

[16] Y. Sota , O. Iguchi, M. Morikawa and T.Tatekawa and K.Maeda, 2001, astro-ph0009412